

# Full-Spectrum Neuronal Diversity and Stereotypy through Whole Brain Morphometry

Yufeng Liu<sup>1</sup>, Shengdian Jiang<sup>1,†</sup>, Yingxin Li<sup>1,†</sup>, Sujun Zhao<sup>1,‡</sup>, Zhixi Yun<sup>1,‡</sup>, Zuo-Han Zhao<sup>1,‡</sup>, Lingli Zhang<sup>1</sup>, Gaoyu Wang<sup>1</sup>, Xin Chen<sup>1</sup>, Linus Manubens-Gil<sup>1</sup>, Yuning Hang<sup>1</sup>, Qiaobo Gong<sup>1</sup>, Yuanyuan Li<sup>2</sup>, Penghao Qian<sup>1</sup>, Lei Qu<sup>1,2</sup>, Marta Garcia-Forn<sup>3,4,5,6,7</sup>, Wei Wang<sup>8,9</sup>, Silvia De Rubeis<sup>3,4,5,6,7</sup>, Zhuhao Wu<sup>8,9,10</sup>, Pavel Osten<sup>11</sup>, Hui Gong<sup>12</sup>, Michael Hawrylycz<sup>13</sup>, Partha Mitra<sup>11</sup>, Hongwei Dong<sup>14</sup>, Qingming Luo<sup>15,16</sup>, Giorgio A. Ascoli<sup>17</sup>, Hongkui Zeng<sup>13</sup>, Lijuan Liu<sup>1</sup>, Hanchuan Peng<sup>1,\*</sup>

<sup>1</sup> New Cornerstone Science Laboratory, SEU-ALLEN Joint Center, Institute for Brain and Intelligence, Southeast University, Nanjing, Jiangsu, China

<sup>2</sup> Ministry of Education Key Laboratory of Intelligent Computation and Signal Processing, Information Materials and Intelligent Sensing Laboratory of Anhui Province, School of Electronics and Information Engineering, Anhui University, Hefei, Anhui, China

<sup>3</sup> Seaver Autism Center for Research and Treatment, Icahn School of Medicine at Mount Sinai, New York, NY, USA

<sup>4</sup> Department of Psychiatry, Icahn School of Medicine at Mount Sinai, New York, NY, USA

<sup>5</sup> The Mindich Child Health and Development Institute, Icahn School of Medicine at Mount Sinai, New York, NY, USA

<sup>6</sup> Friedman Brain Institute, Icahn School of Medicine at Mount Sinai, New York, NY, USA

<sup>7</sup> Alper Center for Neural Development and Regeneration, Icahn School of Medicine at Mount Sinai, New York, NY 10029, USA

<sup>8</sup> Appel Alzheimer's Disease Research Institute, Feil Family Brain and Mind Research Institute, Weill Cornell Medicine, New York, NY 10021, USA

<sup>9</sup> Department of Cell, Developmental & Regenerative Biology, Icahn School of Medicine at Mount Sinai, New York, NY, USA

<sup>10</sup> Department of Neuroscience, Icahn School of Medicine at Mount Sinai, New York, NY, USA  
<sup>11</sup> Cold Spring Harbor Laboratory, Cold Spring Harbor, NY, USA

<sup>12</sup> HUST-Suzhou Institute for Brainsmatics, JITRI, Suzhou, China

<sup>13</sup> Allen Institute for Brain Science, Seattle, WA, USA

<sup>14</sup> Center for Integrative Connectomics, Department of Neurobiology.

Los Angeles, CA, USA

<sup>15</sup> State Key Laboratory of Digital Medical Engineering, School of Biomedical Engineering, Hainan University, Haikou, China.

<sup>16</sup> Key Laboratory of Biomedical Engineering of Hainan Province, One Health Institute, Hainan University, Haikou, China.

<sup>17</sup> Volgenau School of Engineering, George Mason University, Fairfax, VA, USA

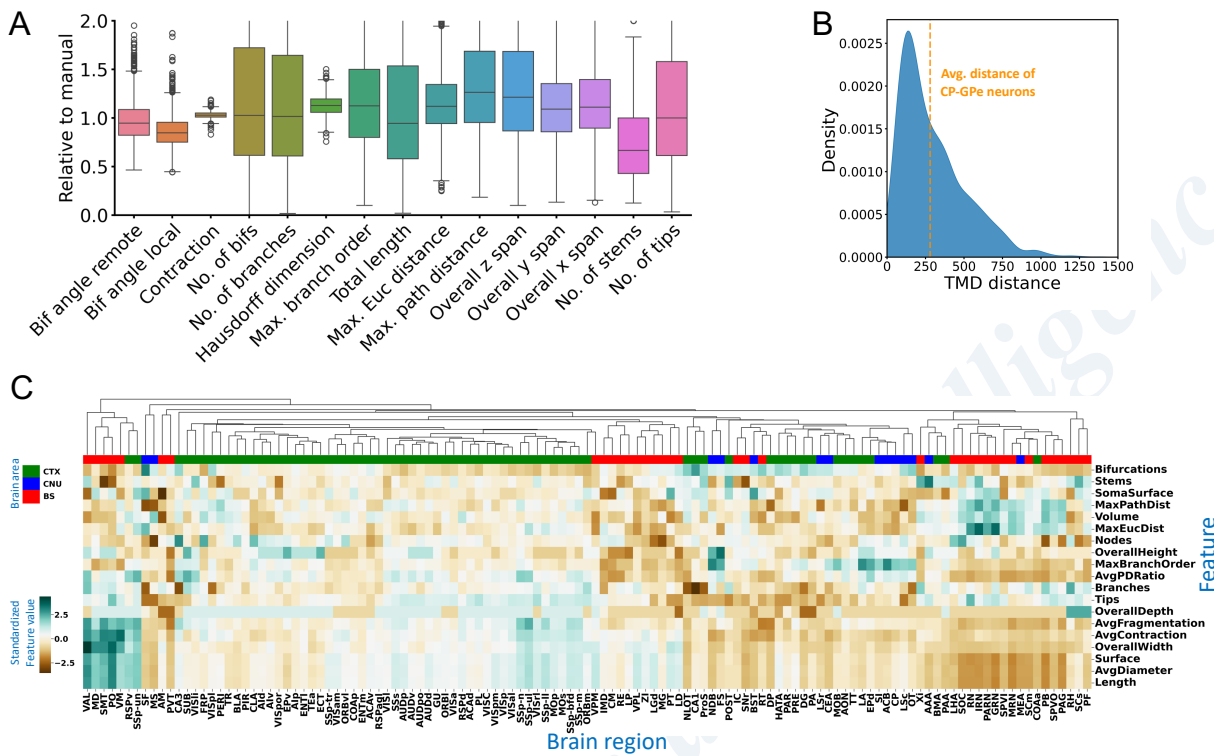
<sup>†</sup>These authors contributed equally.

<sup>†</sup>These authors contributed equally.

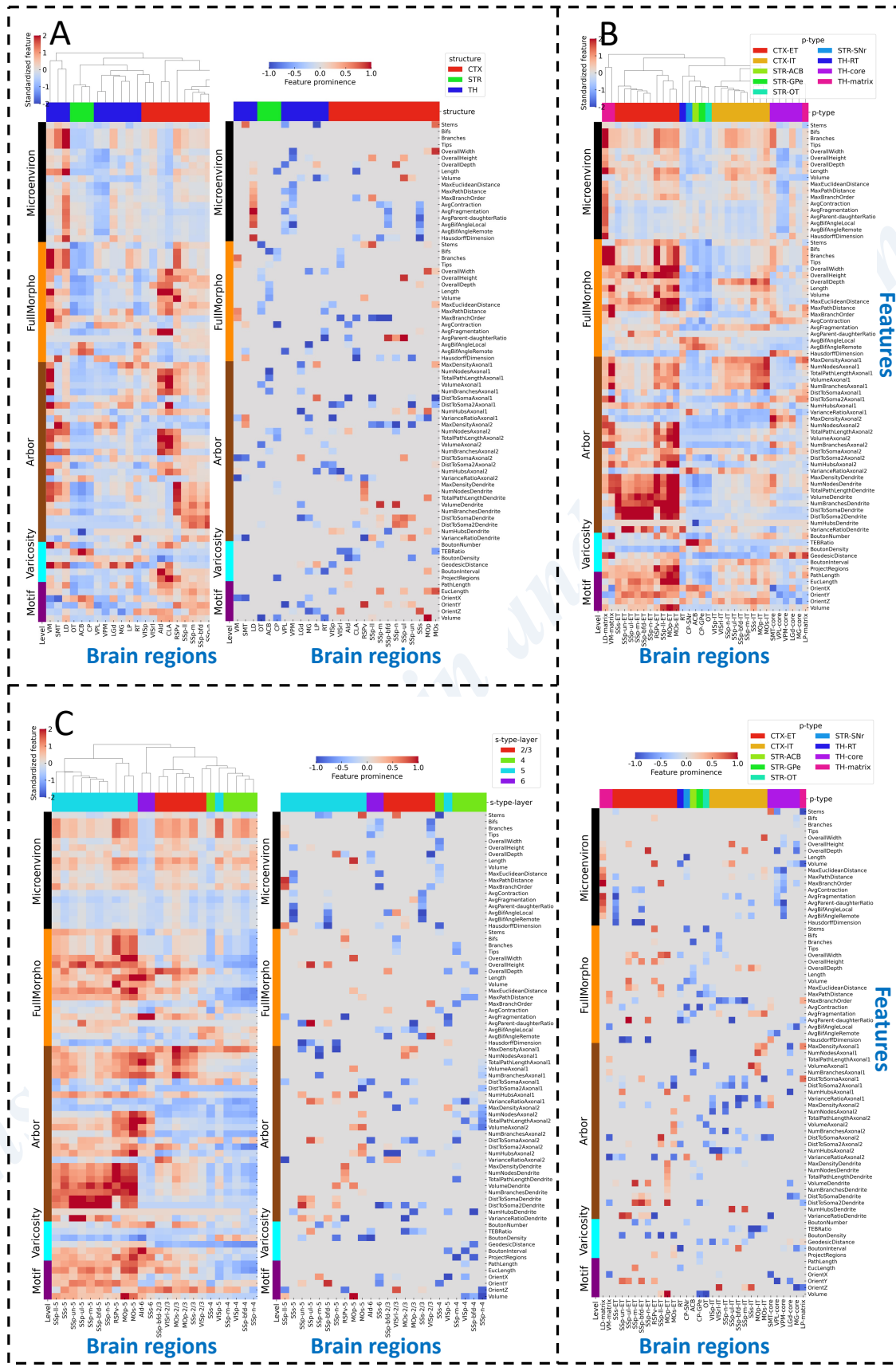
\*Correspondence: h@haintell.org

Correspondence: [n@brainlet.org](mailto:n@brainlet.org)

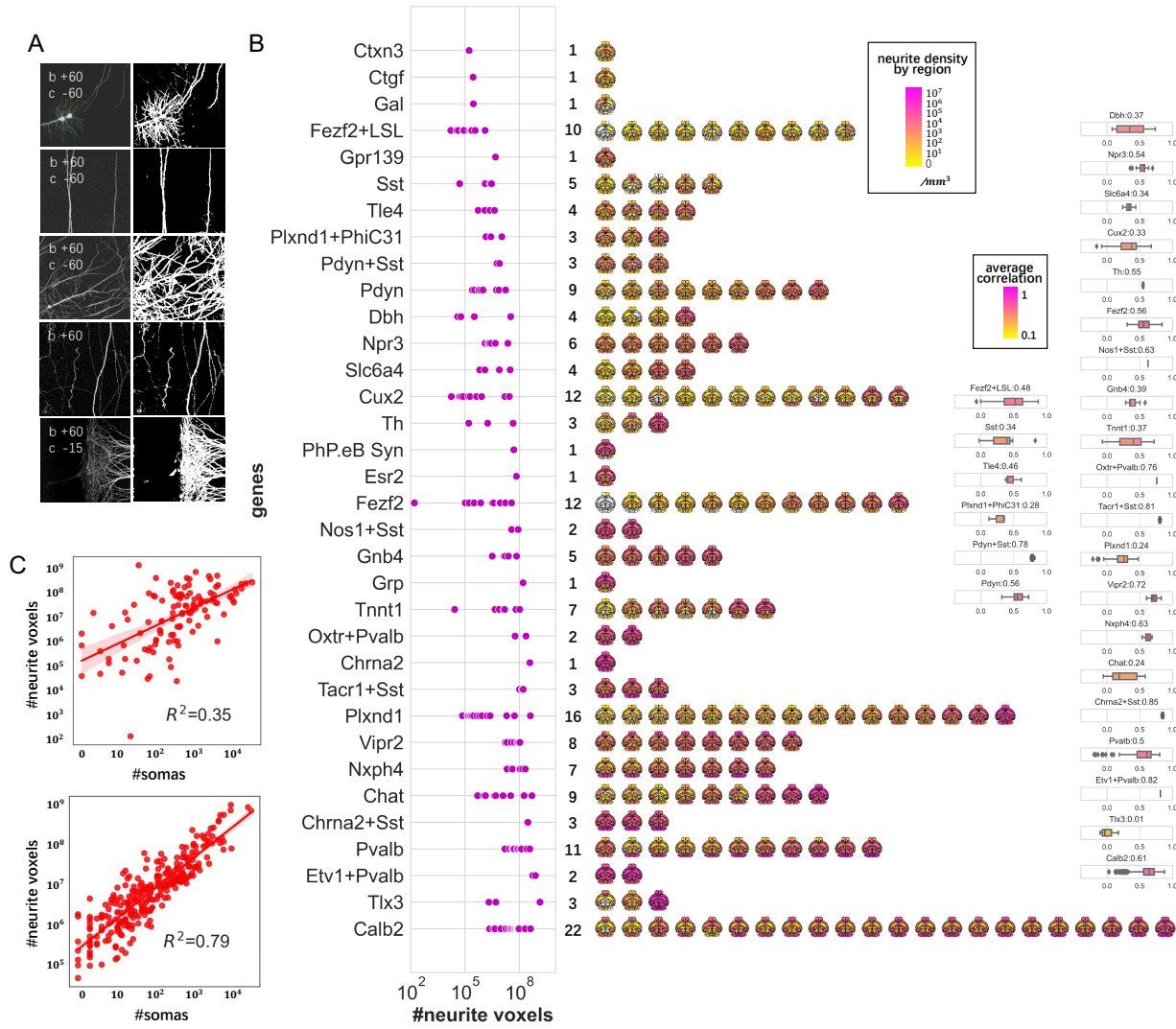
## 47 Supplementary Figures



**Supplementary Figure S1. Verification of the auto-traced local morphologies based on L-Measure<sup>Vaa3D</sup> features.** A. Box plots of the 15 L-Measure<sup>Vaa3D</sup> features. We computed the relative feature values by comparing automated reconstruction to manually annotated local dendrites for each neuron within image blocks of  $512 \times 512 \times 256$  voxels (approximately  $236 \times 236 \times 512 \mu\text{m}^3$ ). A total number of 1754 successfully reconstructed local morphologies and their corresponding manual reconstructions were used for comparison. B. Distribution of the Topological Morphology Descriptor (TMD) distances between the automatic reconstructed morphologies and their corresponding manually annotated dendrites. As a reference, we calculated the average TMD distance of 1000 pairs of manually annotated GPe-projecting CP neurons and indicated by the vertical orange line. C. Hierarchical clustering performed for the 121 regions that contained at least 10 neurons. The regions containing less than 10 neurons (somas) were discarded, and all other neurons in the SEU-D15K were used in calculating the regional features, which involved three brain areas consisting of functionally related region sets defined in CCFv3, namely cerebellum (CB), cerebral nuclei (CNU), and cortex (CTX). The regions and brain areas were estimated based on soma location after registration to the CCFv3 atlas. The corresponding brain area for each region was listed at the top of the heatmap. The regional features were represented by the median features of all neuronal 19-dimensional L-Measure<sup>Vaa3D</sup> features in the corresponding regions. The values of each feature were Z-score normalized separately. The neuronal features exhibited a notable aggregation according to brain areas in general.

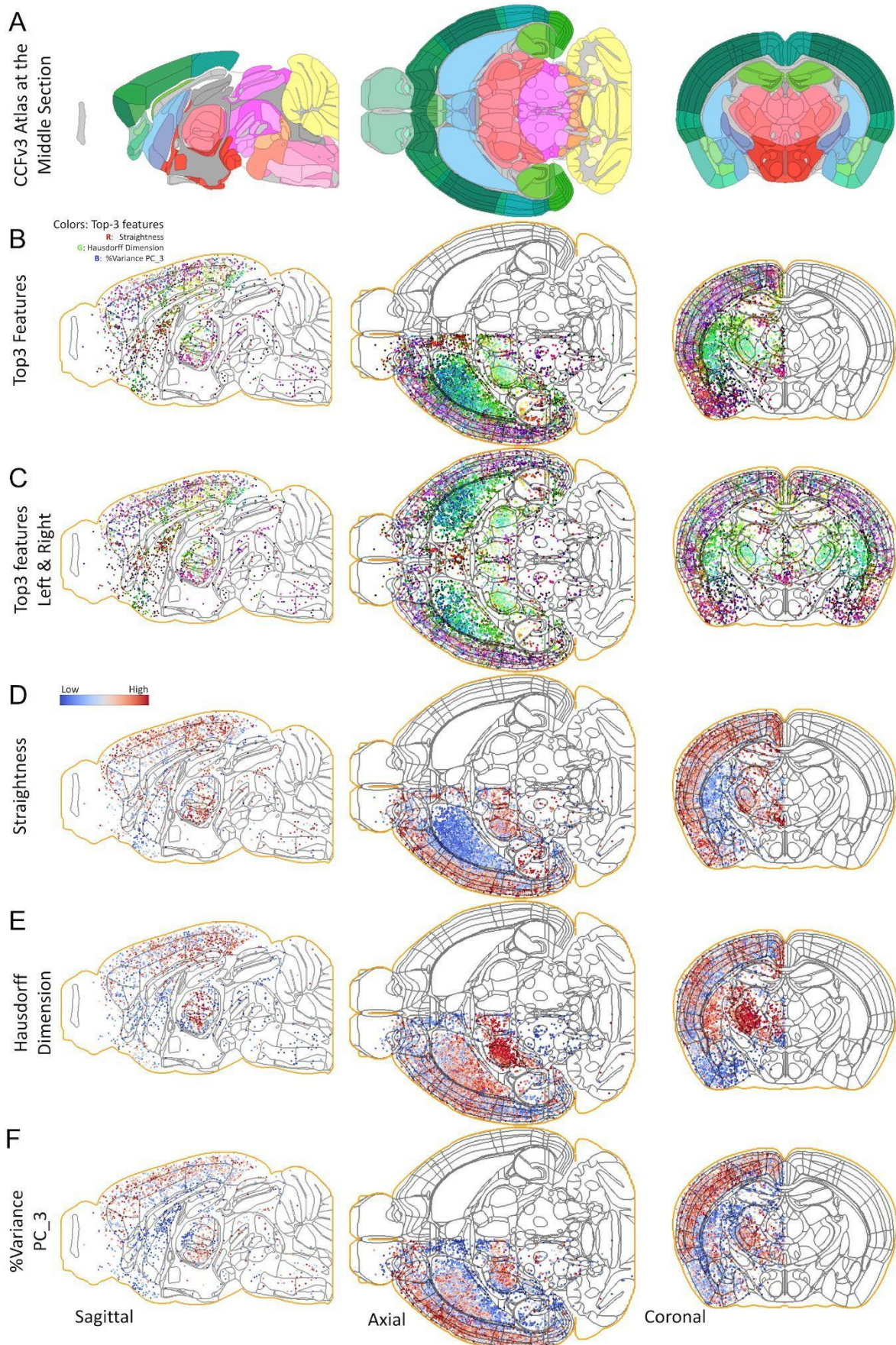


67 **Supplementary Figure S2. Cross-scale feature maps of whole-brain neuron types and subtypes.** **A.** Left: Cross-  
 68 scale feature map for soma types (s-types) that incorporates five different scales: microenvironment, full morphology,  
 69 arbor, varicosity, and motif. By combining these features, a comprehensive set of cross-scale features is obtained. The  
 70 values of each feature are Z-score normalized by subtracting their mean value and then dividing by their standard  
 71 deviation. The right and left y-ticks of the map are the feature names and their corresponding morphometry levels,  
 72 respectively. Hierarchical clustering is applied to all s-types, and the resulting dendrogram is displayed at the top of  
 73 the map. The x-ticks are sorted according to the dendrogram. Right: The feature prominence map delineates the ten  
 74 most discriminating features for each s-type, with the prominence scores determined by the ordering of the absolute  
 75 feature values, and subsequently max-normalized by dividing 10. The prominence values are colored by the signs of  
 76 their original features value in the cross-scale feature map, with blue indicating a positive value and red indicating a  
 77 negative value. **B-C** are similar maps for projection subtypes (sp-types) and lamination subtypes (sl-types) of cortical  
 78 neurons, where ET and IT are the extratelencephalic and intratelencephalic projecting subtypes, and 2/3, 4, 5, 6 are  
 79 the cortical layers of somas.

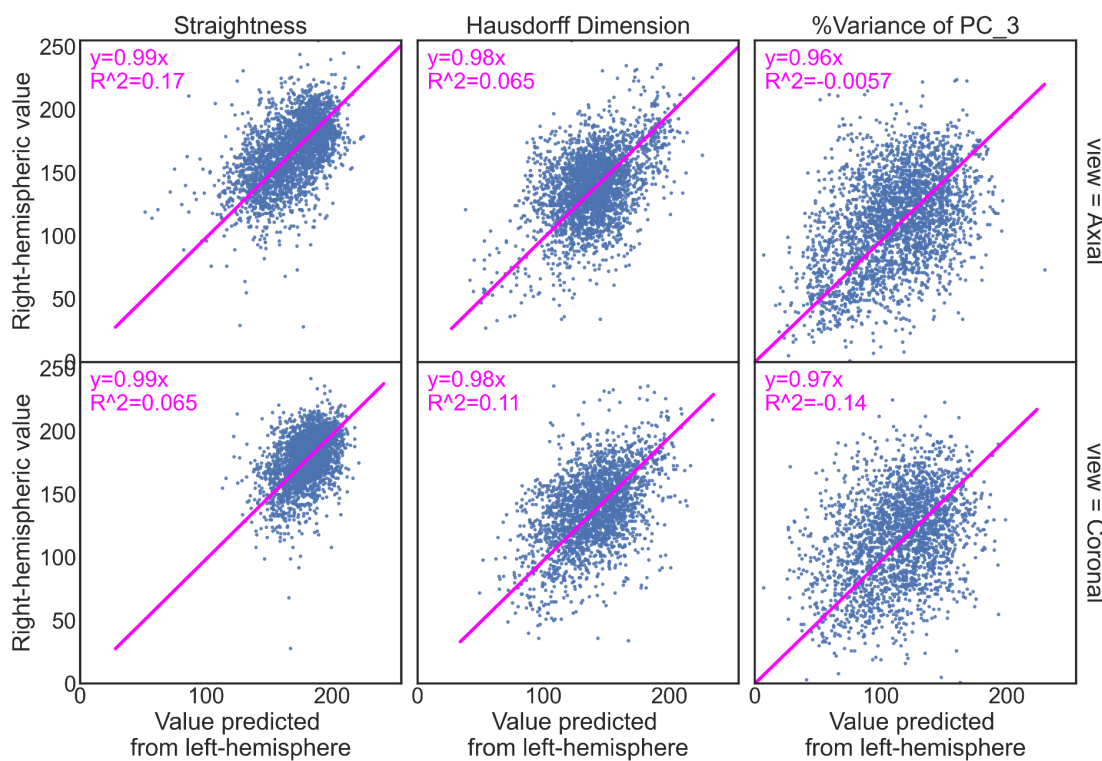


80 **Supplementary Figure S3. The neurite voxel distributions in fMOST brains.** **A.** Image blocks exemplifying our  
 81 neurite segmentation results in fMOST brains. The left and right images are the maximum intensity projections (MIP)  
 82 of raw images and corresponding neurite segmentation maps. The top left legends on the raw MIPs are the adjustments  
 83 applied on them for better visualization. ‘b’ and ‘c’ represent brightness and contrast adjustment, while ‘+’ and ‘-’  
 84

85 signify percentage changes for the corresponding adjustments. **B.** Distributions of neurite voxel numbers of 183 brains  
86 from 34 driver genes. The number of neurite voxels is the total number of voxels identified in a brain image. Each  
87 magenta dot represents a brain, and the total number of brains in each line is displayed on the right side. **C.** Whole-  
88 brain neurite patterns. Zoom-out view of whole-brain neurite voxel distribution at a regional level. Box plots on the  
89 right side show the correlations between regional neurite distribution patterns of all brain pairs in each transgenic line.  
90 **D.** Top: Relationship between the number of identified neurite voxels and the total number of annotated somas for  
91 each brain. Bottom: Relationship between the number of identified neurite numbers and the total number of annotated  
92 somas for every region.

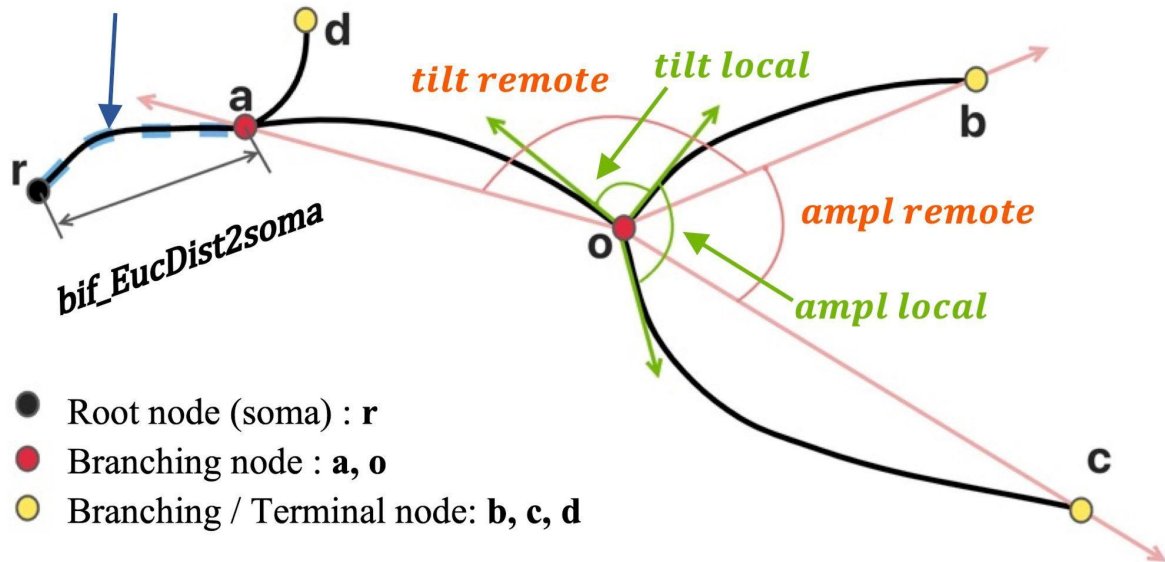


94 **Supplementary Figure S4. Whole-brain microenvironment feature distributions along middle sections of the**  
 95 **sagittal, axial, and coronal views.** **A.** The sagittal, axial, and coronal middle sections of the CCFv3 atlas. Brain areas  
 96 and regions are colored following the convention of the CCFv3 atlas. Cortical regions are in green-blue colors, cerebral  
 97 nuclei regions are in cyan, brain stem regions are in red, midbrain regions are in pink, and cerebellar regions are in  
 98 yellow. The gray lines are the boundaries of CCFv3 regions. **B.** Projection of the top 3 discriminating morphological  
 99 microenvironment features selected through minimum Redundancy-Maximum Relevance (mRMR) on the middle  
 100 sections. The top 3 features are: average straightness, Hausdorff Dimension, and variance percentage of the third  
 101 component of all nodes, and they are encoded in the red (R), green (G), and blue (B) channels of the image. The  
 102 feature values are normalized and histogram-equalized to the unsigned 8-bit integer range. Only neurons within a 1-  
 103 millimeter range in both directions are included. The outermost boundary of the CCFv3 brain template is outlined in  
 104 orange, and the microenvironments on the right hemisphere are flipped to the left hemisphere. **C.** Similar to panel B,  
 105 but the right hemispheric microenvironments are not flipped. **D-F,** The distributions for the three features are displayed  
 106 separately at each view.  
 107

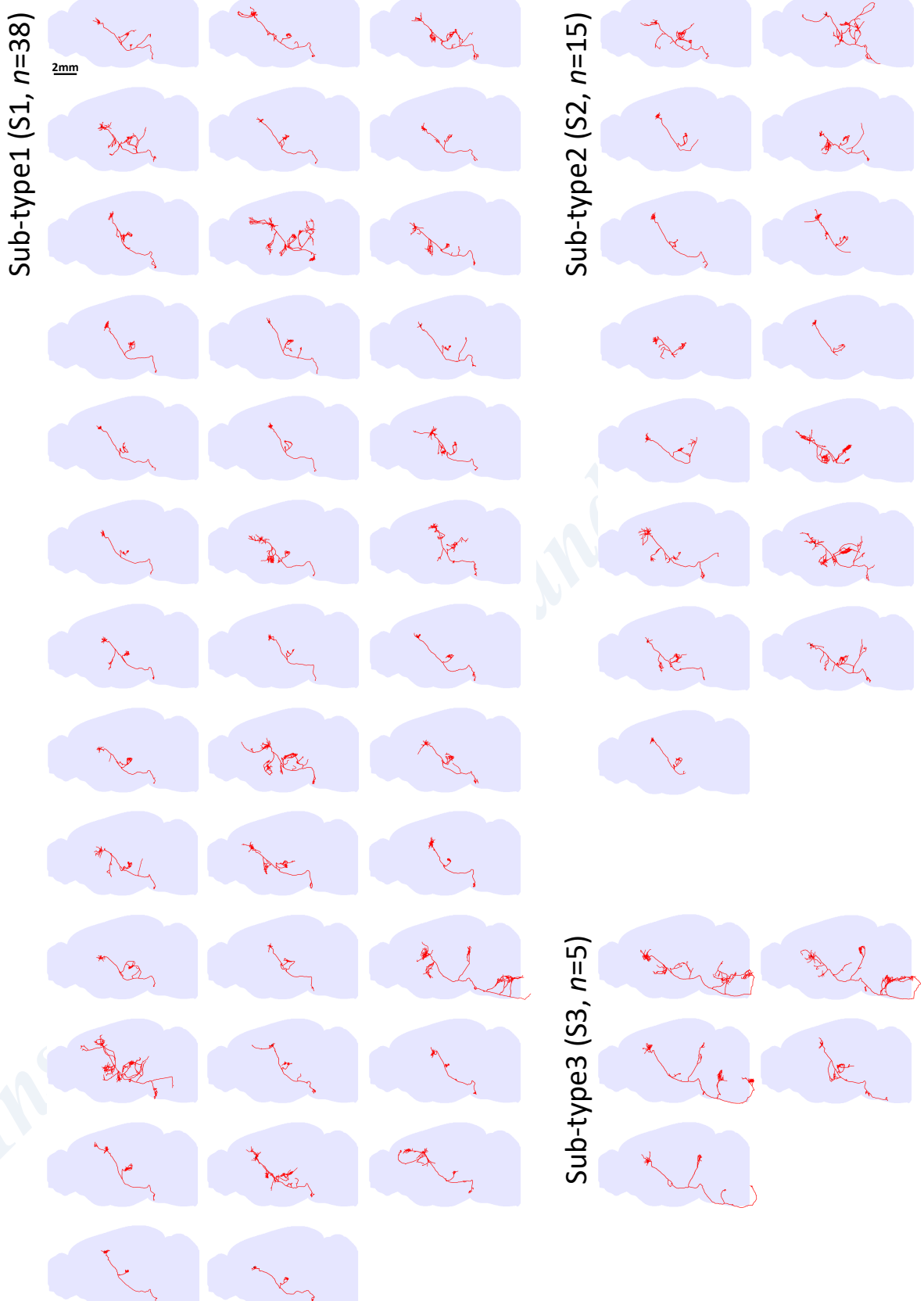


108 **Supplementary Figure S5. Correlations between feature values in the right hemisphere and those predicted**  
 109 **from microenvironments of the left hemisphere on the axial and coronal middle sections.** The values on the y-  
 110 axis are the feature values of microenvironments in the right hemisphere, while the values on the x-axis are predicted  
 111 features for mirrored positions through multidimensional linear interpolation using features of the left hemisphere.  
 112 The points are fitted with the linear function  $y = a \cdot x$ .  
 113

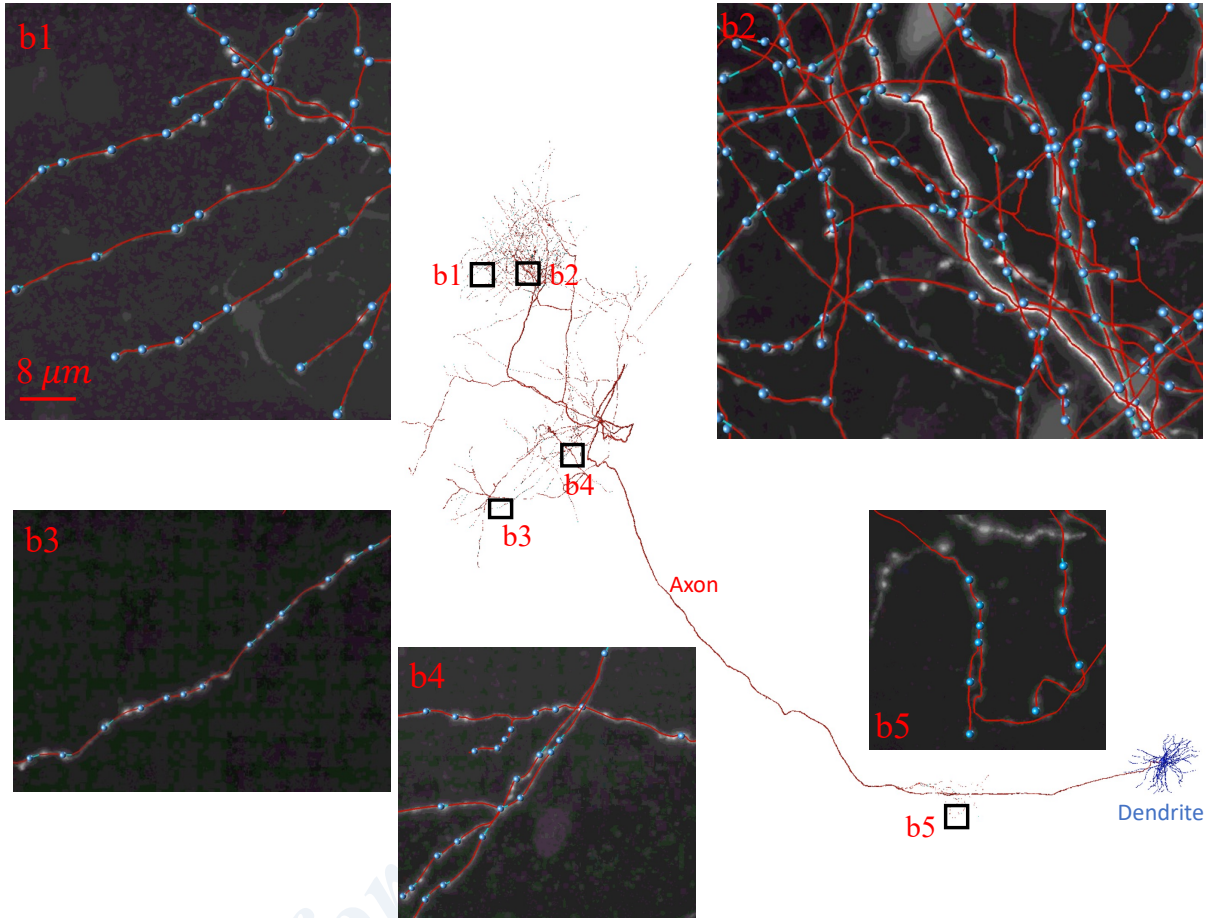
**bif\_PathDist2soma**



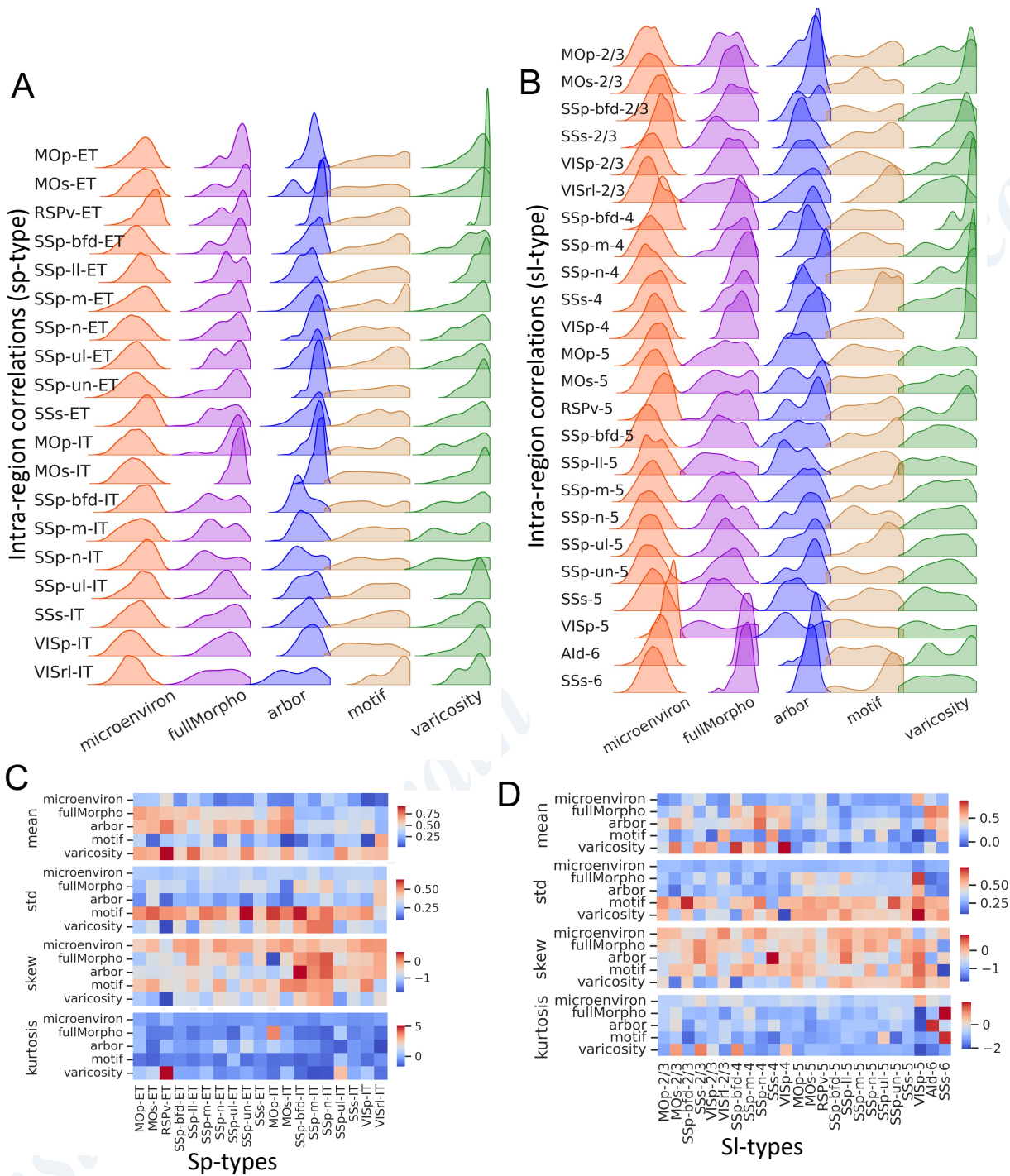
115  
 116 **Supplementary Figure S6.** Diagram illustrating the definition of several critical local morphological features  
 117 leveraged in full morphology analysis. The features ‘bif\_EucDist2soma’ and ‘bif\_PathDist2soma’ are Euclidean  
 118 and path distances from the current bifurcation point to the root node (soma). ‘tilt remote’ is the ‘bif\_tilt\_remote’  
 119 defined in L-Measure<sup>Vaa3D</sup>, which represents the angle between the parent node, the current bifurcation point, and one  
 120 of its two daughter critical nodes. The smaller angle of the two angles formed with the two daughter nodes is used. A  
 121 critical node here is a topological critical point that is either a terminating point, a bifurcation point, or a root point.  
 122 The feature ‘tilt local’ is similar to ‘tilt remote’ except the anchor points are not critical points, but instead are the  
 123 nearest compartments along the branches. The features ‘ampl remote’ and ‘ampl local’ are similar to ‘tilt remote’ and  
 124 ‘tilt local’ except that the angle is formed by daughter points and the current branching point.



126 **Supplementary Figure S7.** Sagittal projections of the three subtypes of L5 ET-projecting SSp-m neurons in the  
127 cortex. L5 ET-projecting SSp-m neuron is a fine-grain extratelencephalic projecting cortical neuron type SSp-m with  
128 the soma located at cortical layer 5 (L5). All 38 subtype-1, 15 subtype-2, and 5 subtype-3 neurons are overlaid on the  
129 sagittal view of the CCFv3 template. The three subtypes are classified based on the terminal coordinates of their  
130 primary tracts using K-Means clustering.

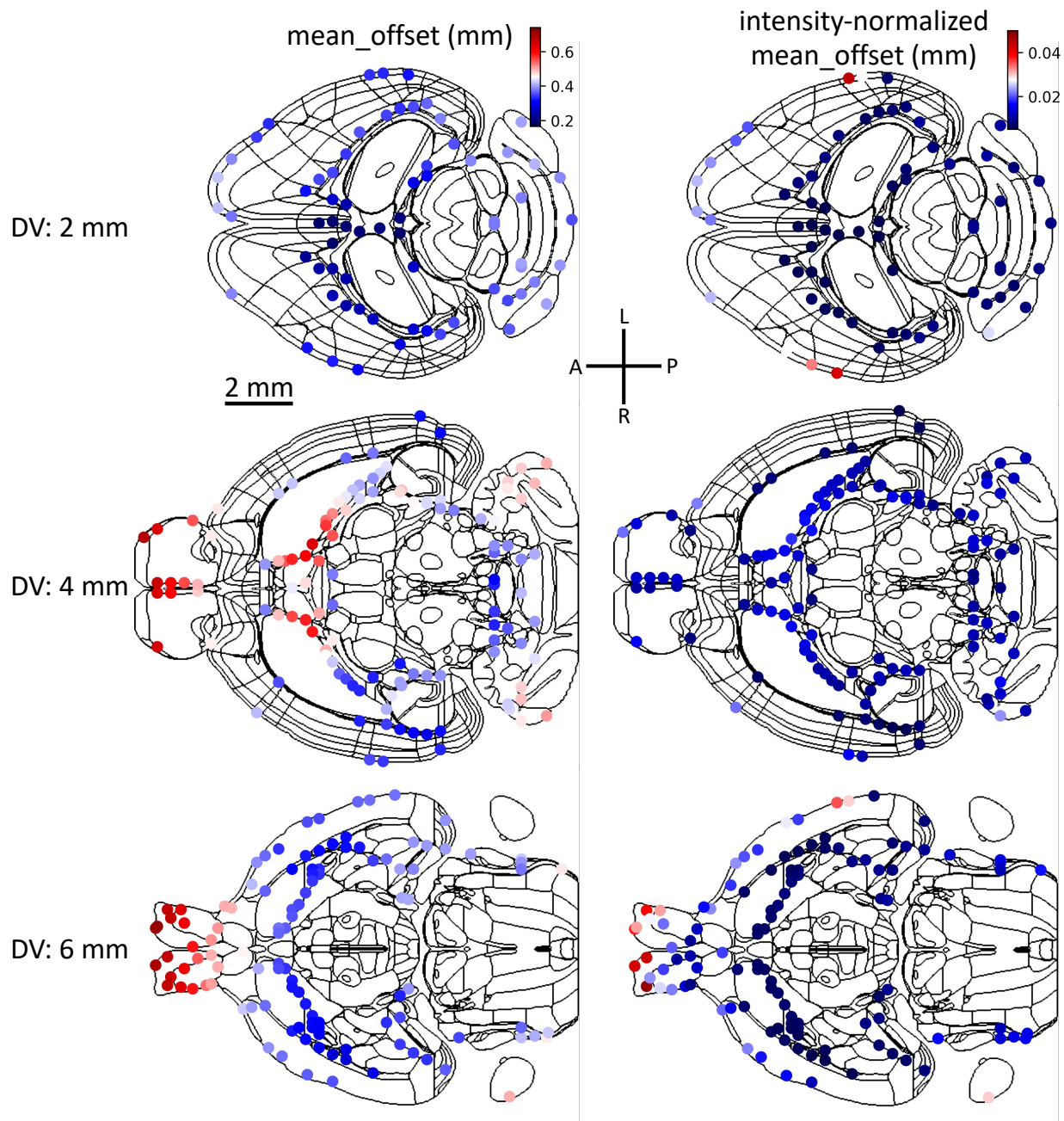


131  
132 **Supplementary Figure S8.** A thalamic VPM neuron with detected varicosities overlaid. Five zoom-in blocks, b1-  
133 5, are displayed through maximum intensity projection (MIP), and the reconstructed skeletons are overlaid in place  
134 with the image. The cyan dots are the detected varicosities. The full morphology of the neuron is illustrated in the  
135 middle of these blocks, with dendrites colored in blue and axons in red.  
136

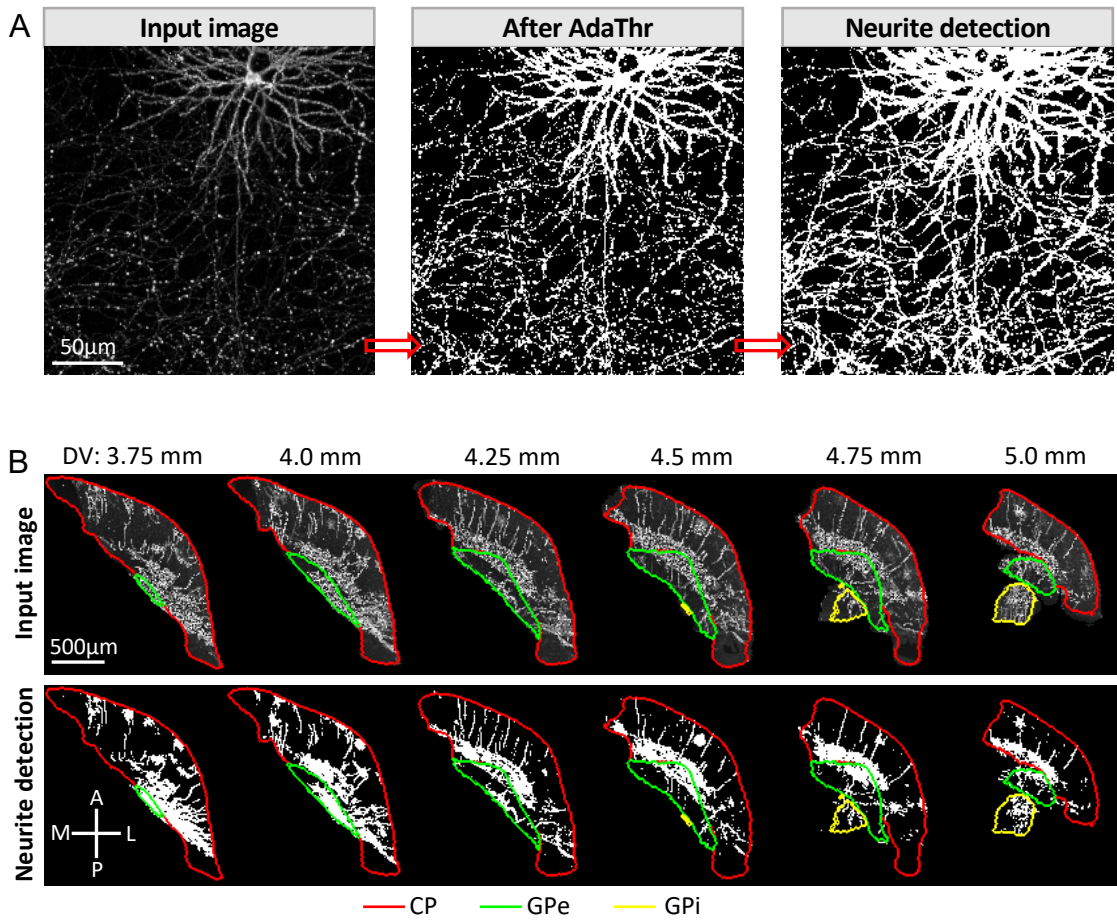


137  
138  
139  
140  
141  
142

**Supplementary Figure S9.** Intra-region correlations for projection subtypes (sp-types) and lamination differentiated subtypes (sl-types) of cortical neurons. **A** and **B**. Density plots of the intra-region correlation distributions for sp-types and sl-types at different morphometry levels. **C** and **D** Heatmap of the first (mean), second (std), third (skew), and fourth (kurtosis)-order statistics of intra-regional correlation distributions for sp-types and sl-types respectively.

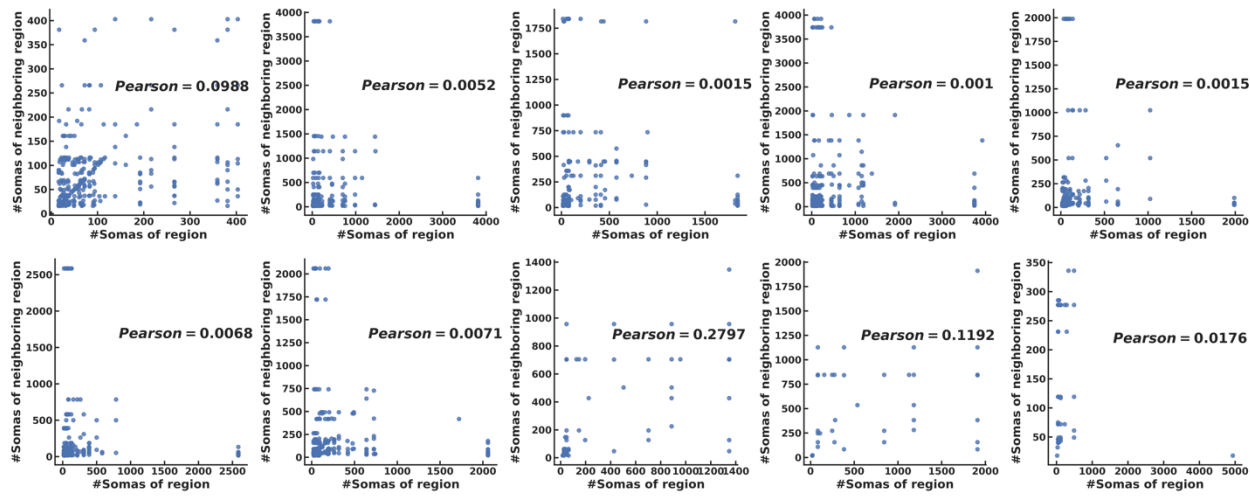


143  
 144 **Supplementary Figure S10. Registration robustness on landmarks.** Three horizontal sections of CCFv3 atlas with  
 145 mean offsets (left) and intensity-normalized mean offsets (right) of landmarks overlaid. The mean offset for each  
 146 landmark was the average offset of that landmark point on all brains analyzed. The intensity-normalized mean offset  
 147 was calculated through dividing the mean offset by the standard deviation of intensities of the mapped landmarks on  
 148 subject brains. To simplify the representation, three horizontal sections along the dorsal-ventral (DV) axis were  
 149 displayed, corresponding to 2, 4, and 6 millimeters from the original point of CCFv3 atlas. Landmarks within 0.25  
 150 millimeters of each section were mapped to that section. Landmarks were color-coded according to their offset values,  
 151 with separate representations for mean offset and normalized offset. The black outlines in each section indicate the  
 152 boundary outlines of the brain regions. Scale bar: 2 mm.  
 153



**Supplementary Figure S11. Neurite detection examples.** **A.** Illustration of neurite detection for a neuronal image block with dendrites and local axons. The first, second, and last columns are the input image, intermediate results after adaptive thresholding filter, and the final neurite detection. Scale bar: 50  $\mu\text{m}$ . **B.** The input neuronal images and corresponding detections for the CP (red), GPe (green), and GPi (yellow) regions. We displayed six sections along the dorsal-ventral (DV) axis, specifically at 3.75 mm, 4.0 mm, 4.25 mm, 4.5 mm, 4.75 mm, and 5.0 mm from the origin point at the dorsal side of the atlas of a fMOST brain. The atlas is reverse-mapped from the CCFv3 atlas based on the registration matrix. Only the regions within the three brain regions (CP, GPe, GPi) are included for visualization. Scale bar: 500  $\mu\text{m}$ .

164



165

### 166 **Supplementary Figure S12. Relationship between the numbers of annotated somas in neighboring regions.**

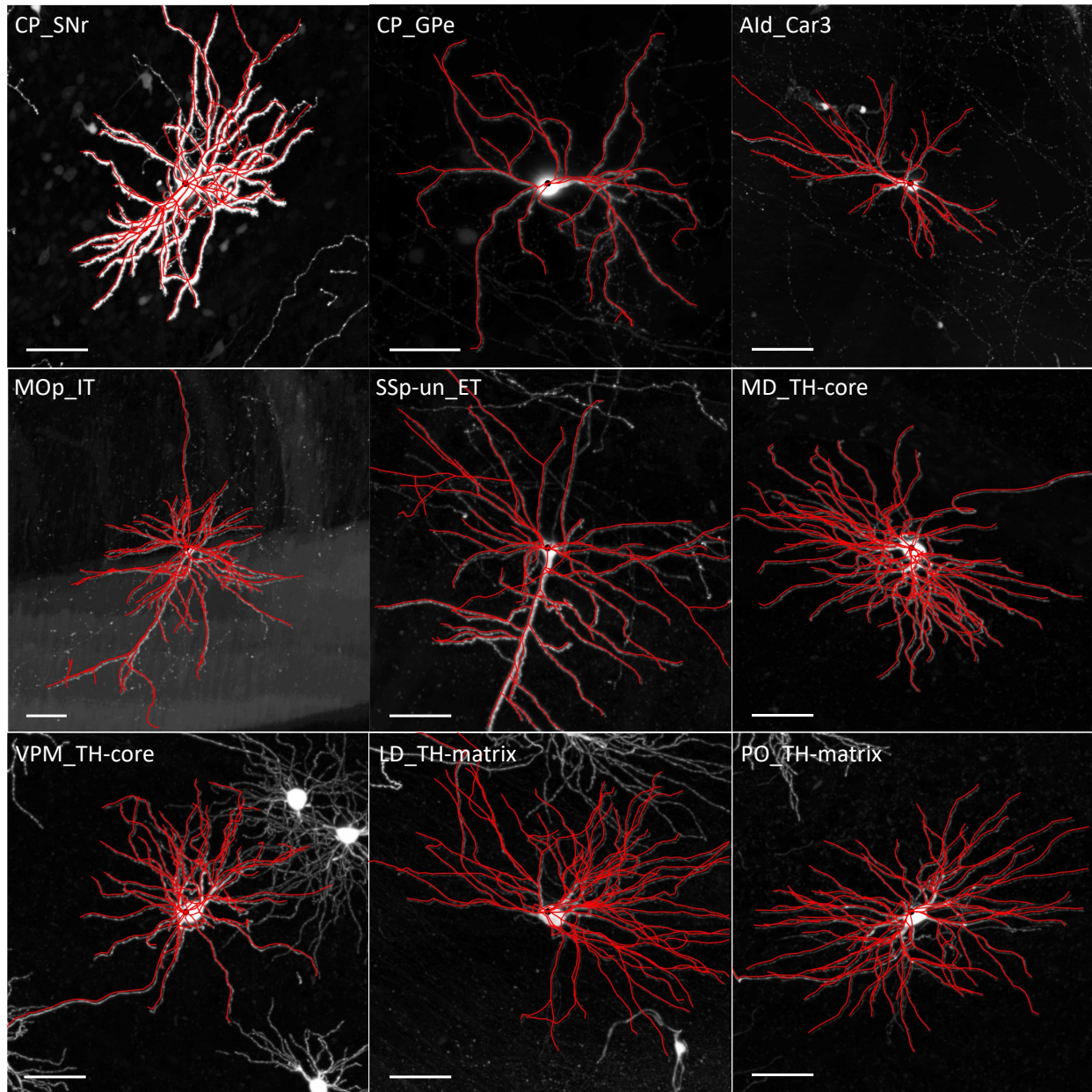
167 Scatter plots of the numbers of somas in neighboring regions for the ten brains with the highest numbers of total  
 168 annotated somas. Each point represents the number of somas annotated in a pair of regions. A region pair is defined  
 169 as two CCFv3 regions with a minimum distance of less than 125  $\mu\text{m}$ . Only regions containing more than 15 somas  
 170 are considered for the sake of statistical reliability. The inset legend in each panel is the Pearson correlation coefficient  
 171 of fitted line (not shown).

172

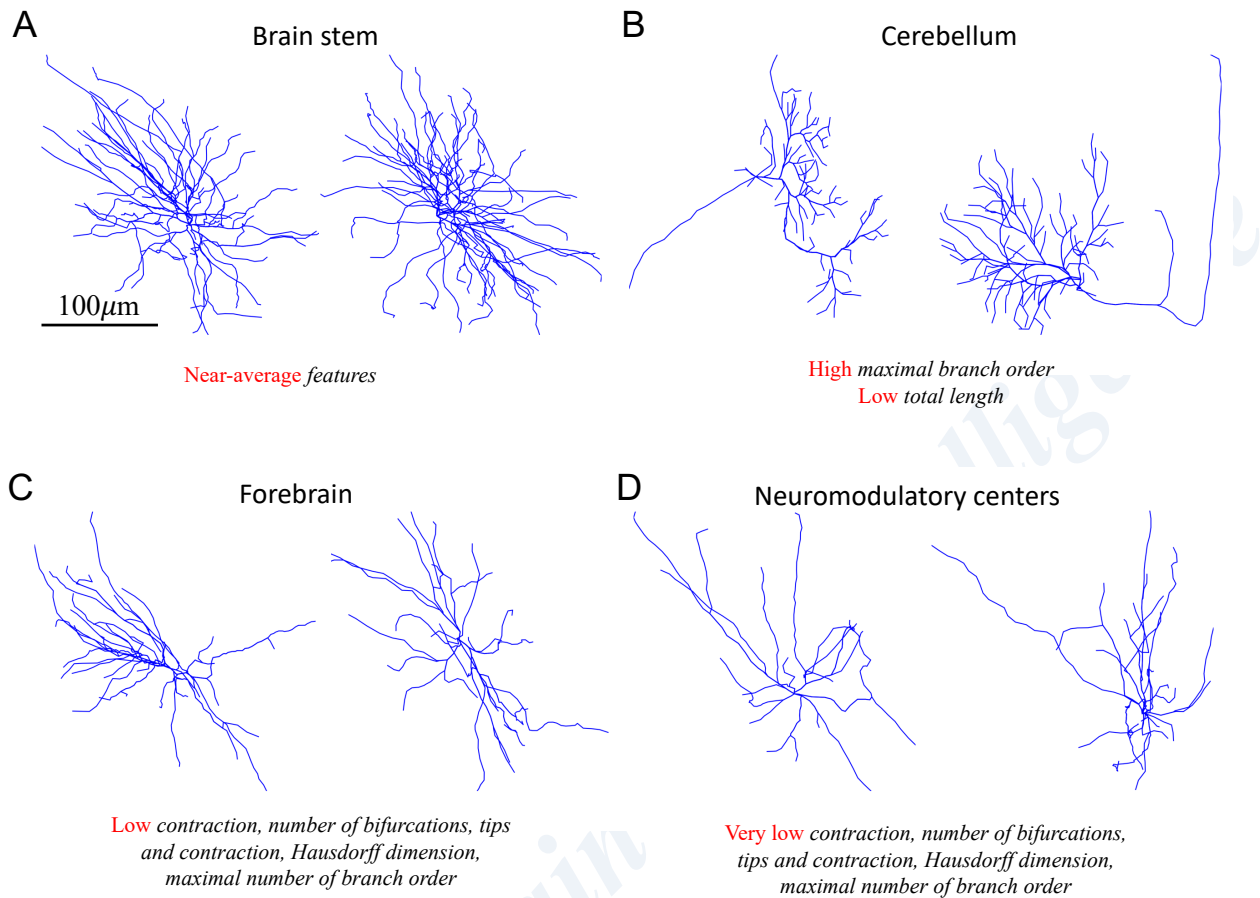
173



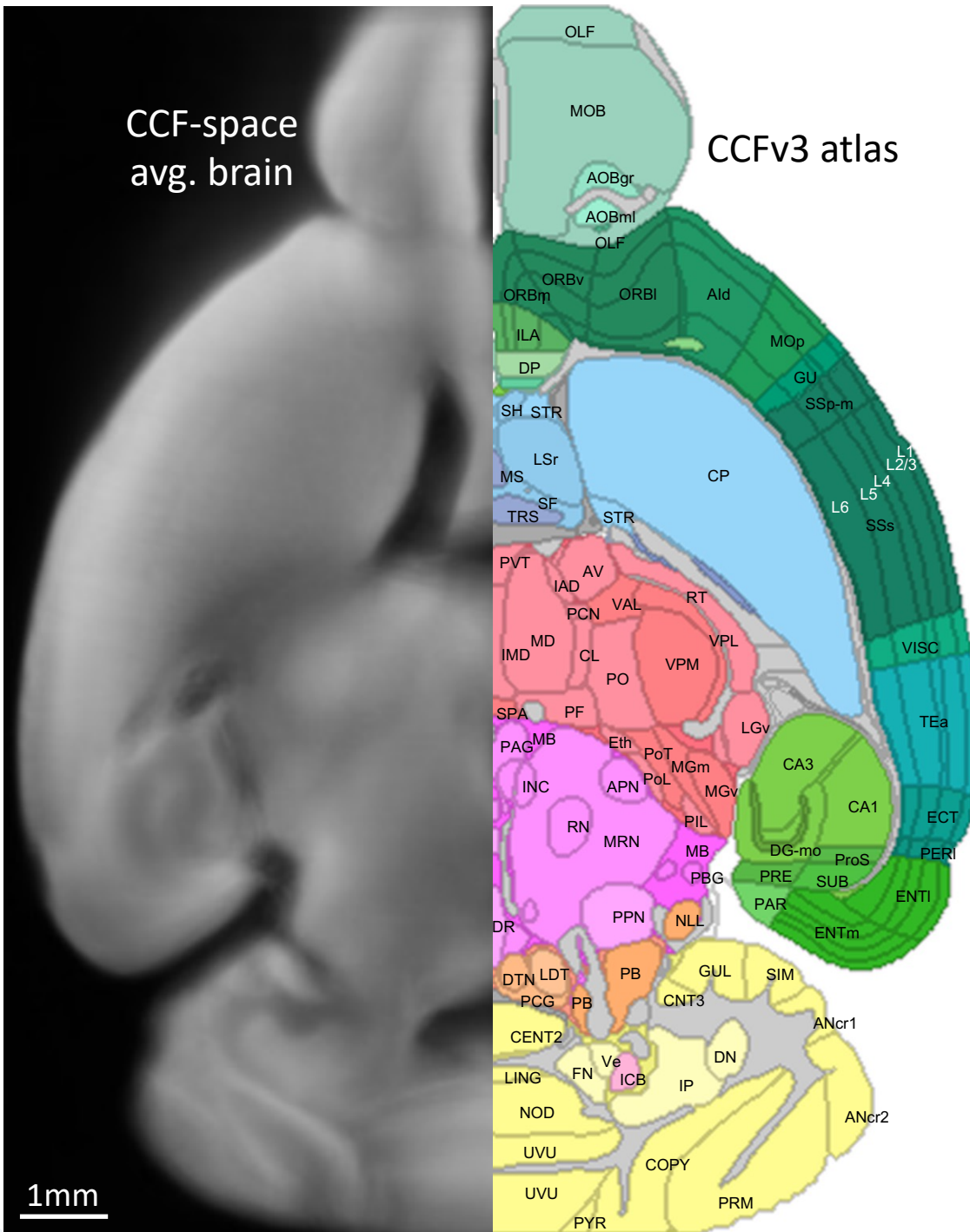
**Supplementary Figure S13. Correlated region sets for 313 brain regions.** Horizontal projections on the CCFv3 template of regions with a Spearman correlation coefficient of at least 0.5 with the target region (specified at the top of each brain image). The box plot on the top of each brain image is the distribution of the pairwise correlations between these regions and the target region, with the box colored by compound areas (CA) as in **Figure 2A**. An intra-CA region set contains only regions from the same compound area, while cross-CA set contains regions from at least two different compound areas.



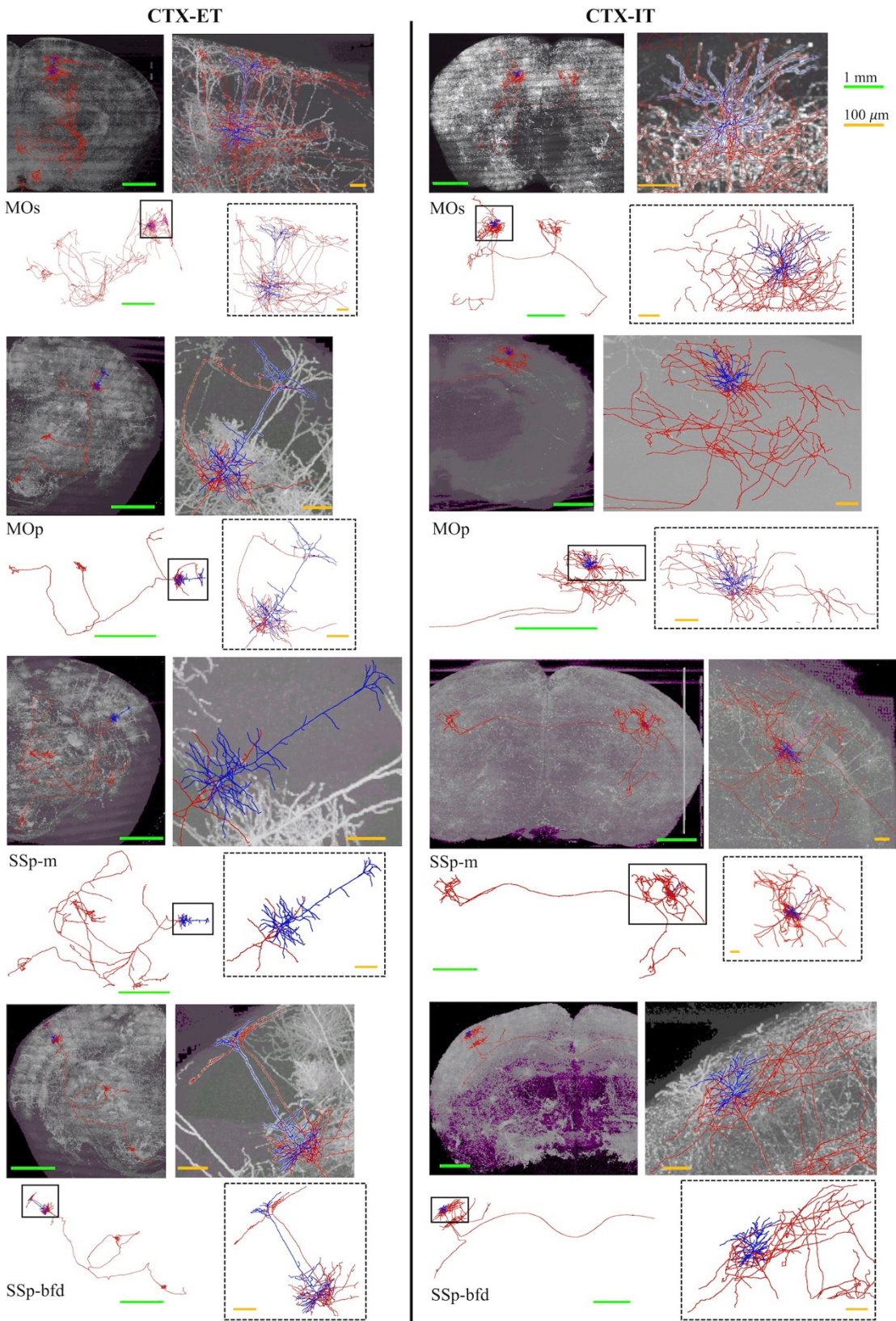
183  
 184 **Supplementary Figure S14.** Examples of automatically reconstructed local dendrites. Nine image blocks from  
 185 different neuron types (or subtypes) are presented. Each neuron is named by concatenating its region name where the  
 186 soma is located and its projection type, separated by an underscore. For instance, CP\_SNr and CP\_GPe refer to SNr  
 187 and GPe-projecting CP neurons, while Ald\_Car3 designates claustrum-like Ald neurons. Additionally, MOp\_IT and  
 188 SSp-un\_ET represent intratelencephalic MOp neurons and extratelencephalic SSp-un neurons, respectively. TH-core  
 189 and TH-matrix refer to the core and matrix projection types. The morphologies are displayed in dots and lines, with  
 190 black dots indicating somas, and red lines representing the fibers. To enhance visualization, the morphologies were  
 191 shifted by 2 voxels horizontally and vertically. Scale bar: 20  $\mu\text{m}$ .  
 192



193  
194 **Supplementary Figure S15. Representative neurons for brain stem, cerebellum, forebrain and neuromodulatory**  
195 **centers.** Sagittal views of the local morphologies of two representative neurons for each brain area are displayed. The  
196 most discriminative L-Measure<sup>Vaa3D</sup> features for each area are summarized below the examples. Scale bar: 100  $\mu\text{m}$ .



197  
 198 **Supplementary Figure S16. The CCF-space average brain.** Left: The middle axial section of the average brain  
 199 generated by averaging 191 whole brain images analyzed in this work. Right: The corresponding axial section of  
 200 CCFv3 atlas with region names explicitly labeled.  
 201



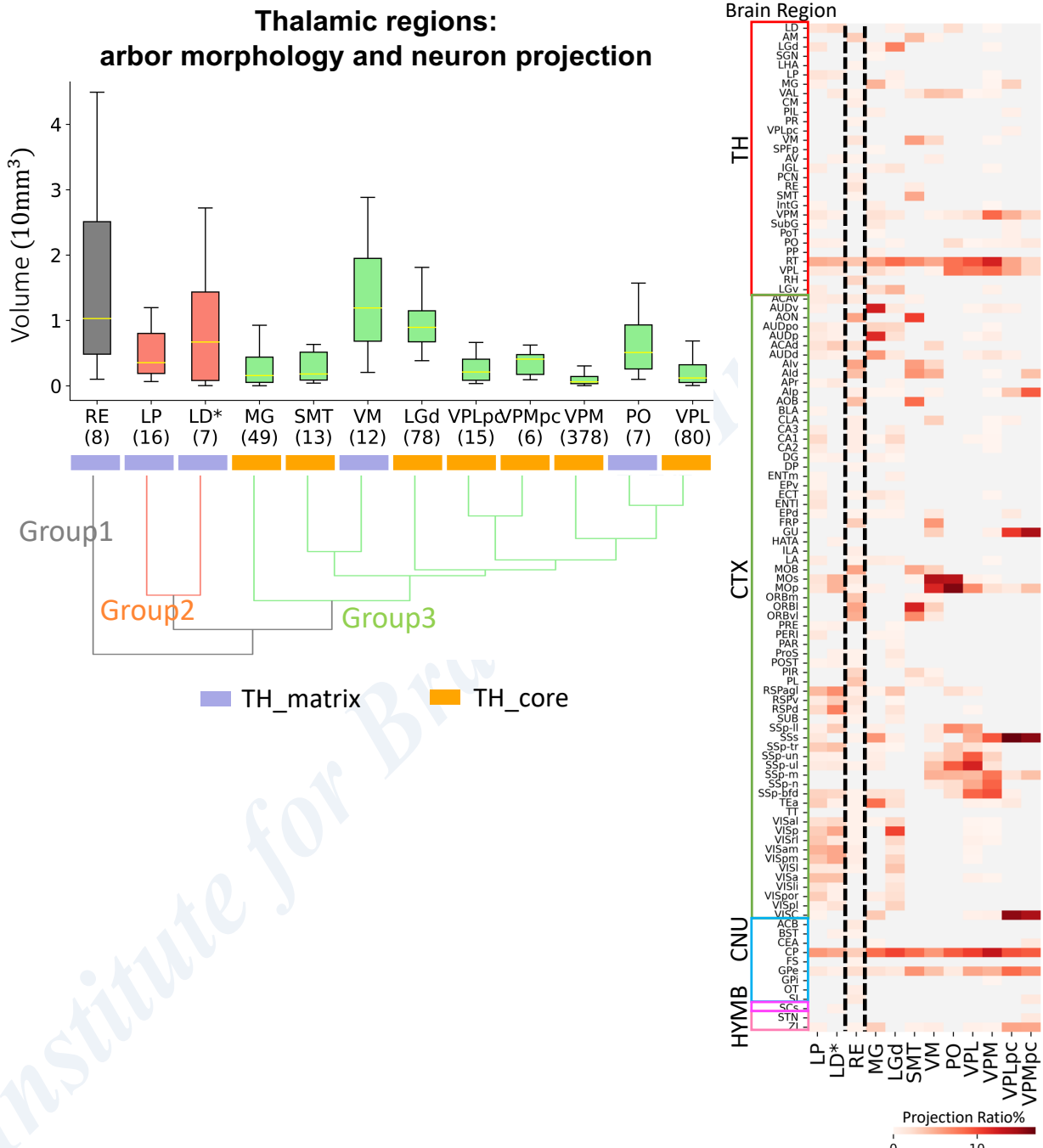
202

203

204

**Supplementary Figure S17. Dendritic arbors of cortical neurons.** Coronal views of dendritic arbors of the ET-projecting (left) and IT-projecting (right) subtypes of four cortical neuron types (MOs, MOp, SSp-m, SSp-bfd). For

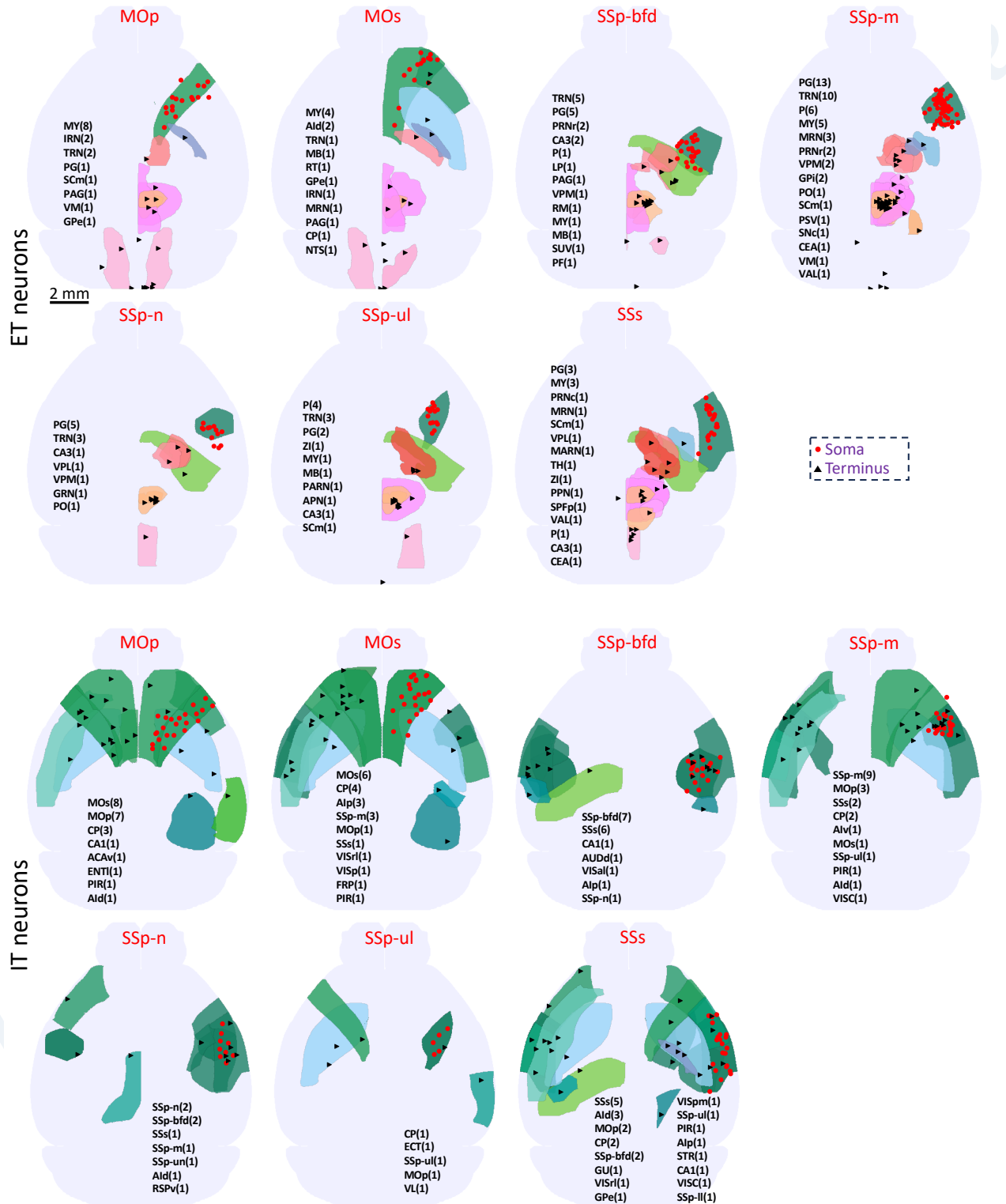
each neuron: top left panel, coronal view of single neuron morphology overlaid on brain image; bottom left, the single neuron morphology, with dendrites highlighted by a solid rectangle; top right, dendrites overlaid on the image; bottom right, dendrites. The morphology is color-coded by the neurite types, with dendrites in blue, and axons in red. Scale bars: green, 1  $\mu$ m; yellow, 100  $\mu$ m.



**Supplementary Figure S18.** Diversity and stereotypy of arbors of thalamic neurons. Left: Box plot showing the arbor volume of 12 thalamic neuron types. The dendrogram shows groups obtained by hierarchical agglomerative clustering based on the combination of 8 morphological features (mean and standard deviation of '#branch', 'volume', 'max\_density', 'dist2soma') and their projection strength vector across the brain regions. Right: Heatmap of the whole-brain projection strength distributions for the 12 types. Each row is a projection region, grouped by their brain

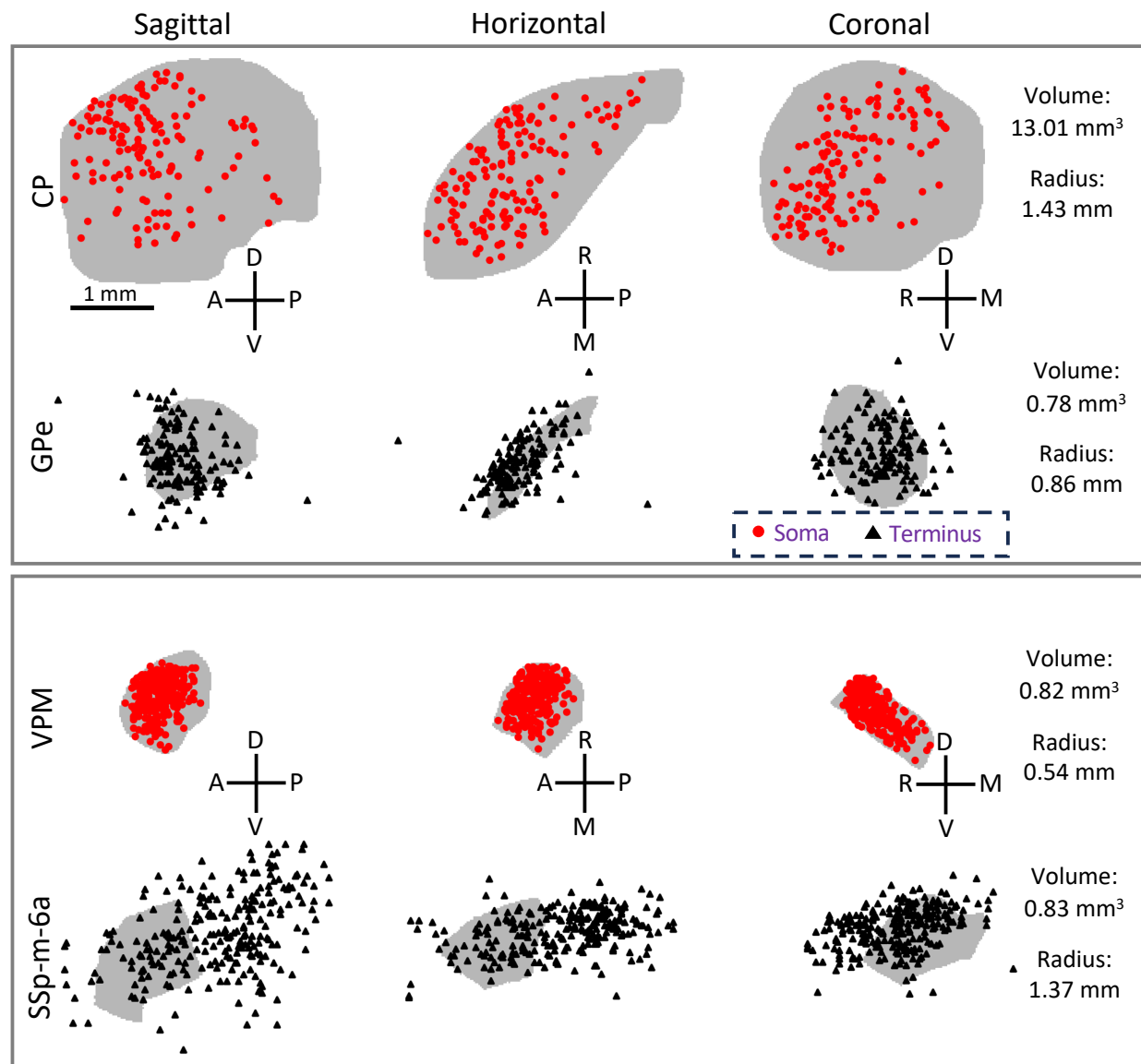
215 areas, which are highlighted at the left of the heatmap. Each row is an s-type region for the analyzed neuron sorted  
 216 according to the clustering results of the left panel. Given that the 'thalamic core' LD neurons only has 3 neurons, the  
 217 projection class 'thalamic matrix' of LD neurons (LD\*) is displayed.

218  
219



220

221 **Supplementary Figure S19.** Projection topographical organizations of the ET and IT projecting neurons of 7  
 222 cortical types. Horizontal views of somas (red dots) and the terminal points of primary axonal tracts (black triangles)  
 223 of neurons belonging to the same projection subtypes are mapped onto the standardized CCFv3 template (ghost white).  
 224 Regions where somas and terminal points located are highlighted with an alpha value of 0.5, color-coded according  
 225 to the CCFv3 atlas. The names of these regions are explicitly provided on the respective brains, with source regions  
 226 in red and terminal regions in black. The number of points within each region is specified in parentheses after the  
 227 region name. Large brain areas, such as medulla (MY), midbrain (MB), pons (P), thalamus (TH), striatum (STR), and  
 228 lateral ventricle (VL), are not shown to avoid obscuring other regions. Scale bar: 5 mm.

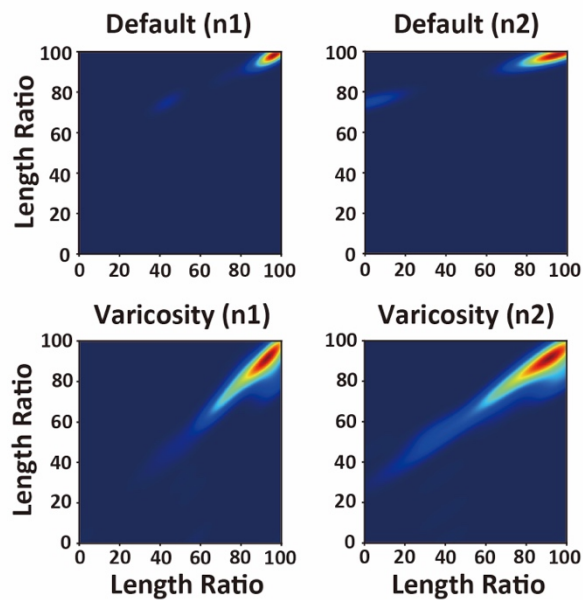
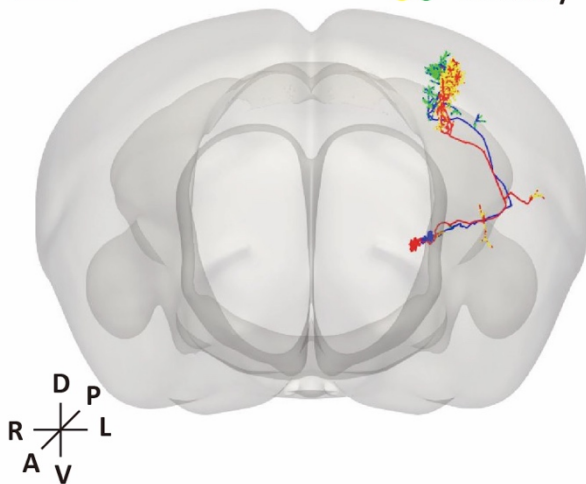


229  
 230 **Supplementary Figure S20.** Projection topography for VPM neurons and GPe-projecting CP neuron. The  
 231 primary sourcing and terminating regions are indicated with light gray mask. Somas and primary axonal tract termini  
 232 are represented by red dots and black triangles, respectively. For each region, sagittal, horizontal, and coronal views  
 233 are provided. Only the regions with the highest number of termini are included. Volumes of regions and radii of somas  
 234 or termini are displayed on the right side. Details on radius calculation can be found in the **Methods** section. Scale  
 235 bar: 1 mm.  
 236

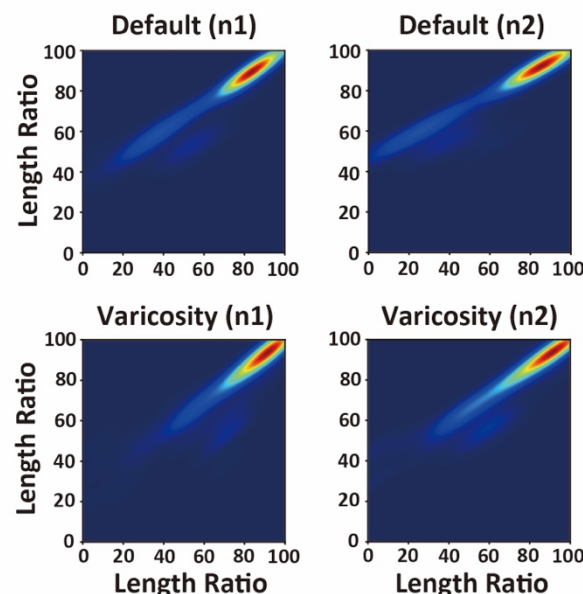
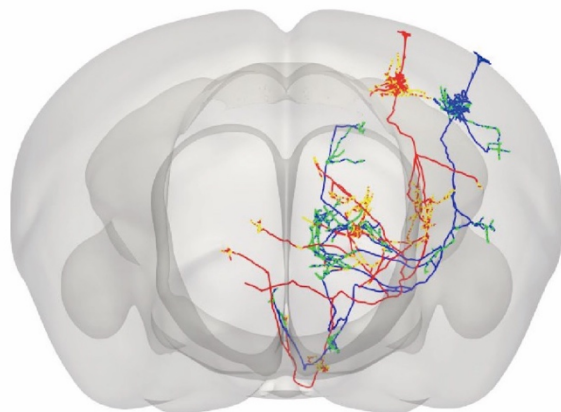
A

**VPL neurons**

1 mm



B

**SSp neurons**

237

238

239

240

241

242

243

244

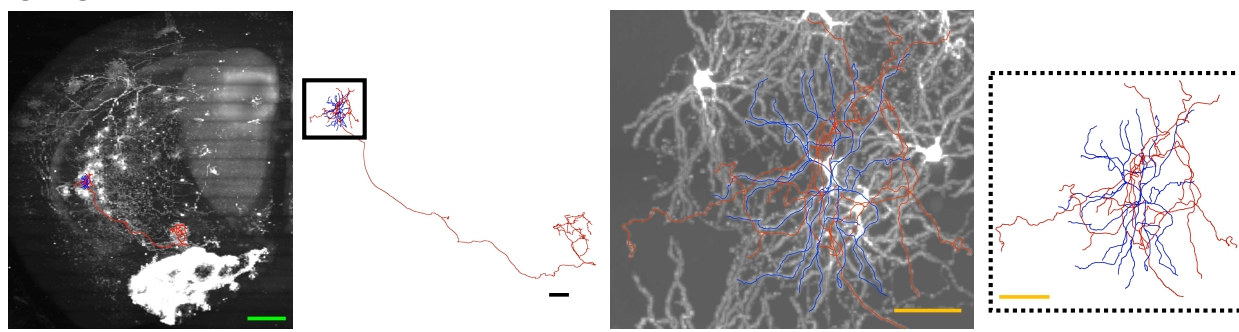
245

246

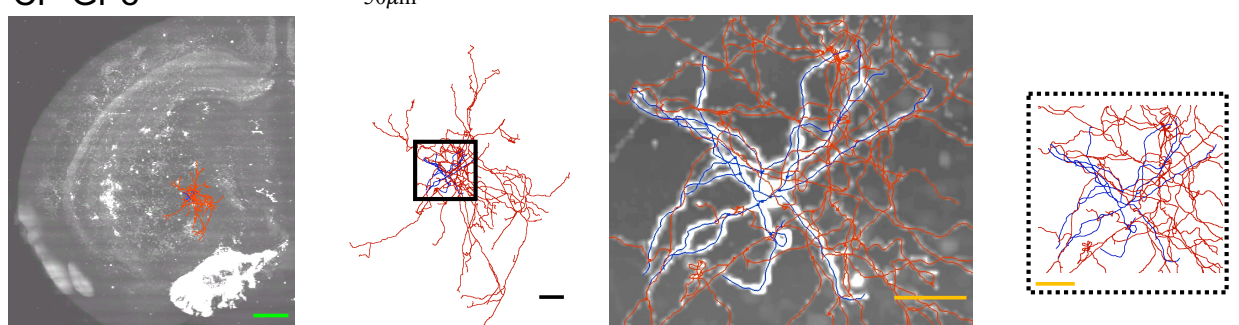
247

**Supplementary Figure S21.** Similar varicosity distributions in morphologically similar neurons. **A.** Left: Coronal view displaying the morphologies of two neurons (neuron 1, n1, in red; neuron 2, n2, in blue) overlaid on the CCFv3 template. Yellow and green dots represent varicosities of neuron 1 and neuron 2, respectively. Right: Heatmap depicting Topological Morphology Descriptor (TMD) persistent lengths for axons (“Default”) and varicosities (“Varicosity”) of the neurons. The lengths represent Euclidean distances between somas and starting points (topologically near the soma, X-axis) or terminal points (topologically far from the soma, Y-axis). Subsequently, these lengths are normalized by the maximum length to create percentiles, referred to as “Length Ratio”. **B.** Comparable components to **A**, but focusing on two morphologically similar neurons from the Primary Somatosensory area (SSp). Scale bar: 1 mm.

CP-SNr

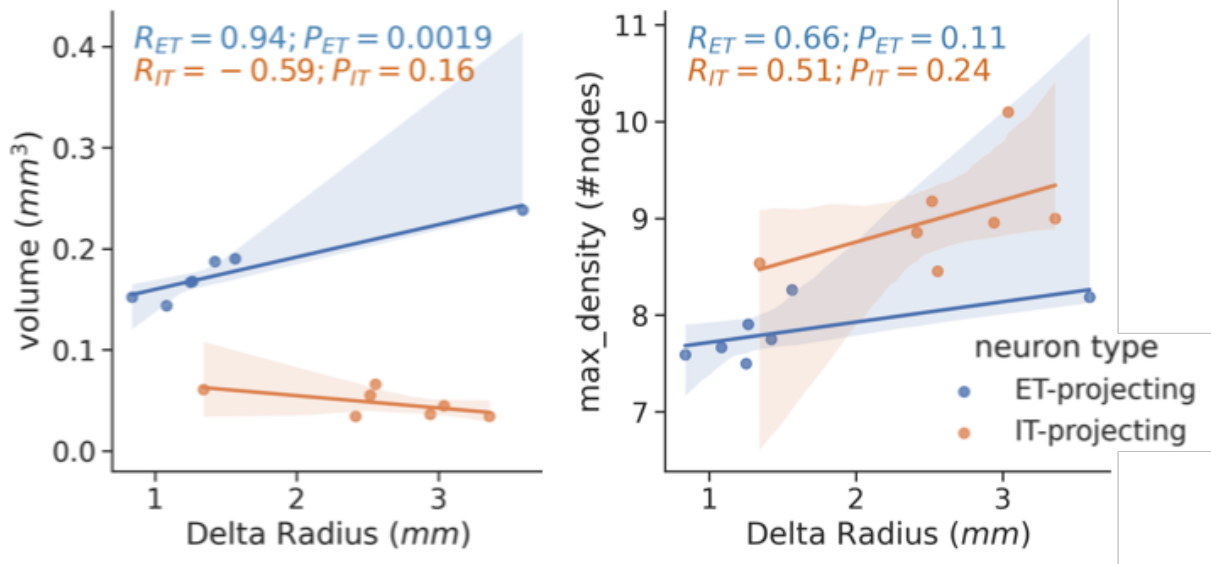


CP-GPe



248  
249  
250  
251  
252  
253

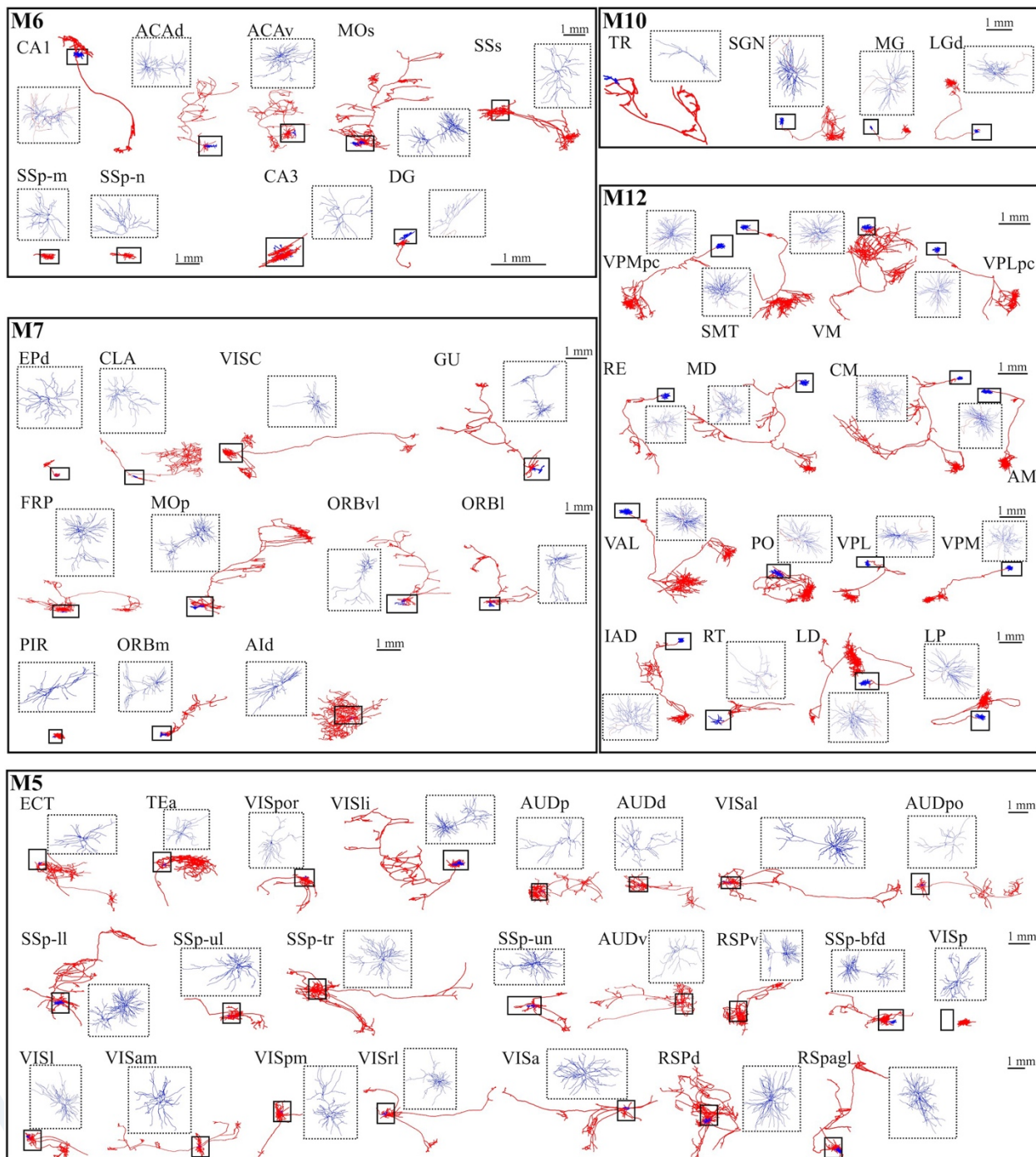
**Supplementary Figure S22. Local axons of CP neurons.** Top panels: coronal views of a SNr-projecting CP neuron; Bottom panels: coronal views of a GPe-projecting CP neuron. From left to right, single neuron morphologies overlaid in the whole brain images, single neuron morphologies with neurites highlighted by black rectangles, zoom-in views of local morphologies overlaid on images, zoom-in views of local morphologies. Neurites are color-coded, with dendrites in blue, and axons in red. Scale bars: green, 500  $\mu$ m; black, 100  $\mu$ m; yellow, 50  $\mu$ m.



254  
255  
256  
257  
258

**Supplementary Figure S23. Cross-scale diversity between dendritic arbors and projection patterns.** The projection patterns are estimated using the Delta Radius, calculated as the radius of primary axonal tract termini minus the radius of the somas for neurons from a given subtype. The feature “volume” represents the total volume of the dendritic arbor. The feature “max\_density” represents the highest density observed among all compartments, with

259 density defined as the count of compartments within a specified neighborhood. Blue dots and orange-yellow dots  
 260 represent extratelencephalic (ET) projecting and intratelencephalic (IT) projecting cortical neurons, respectively. The  
 261 "R" and "P" values represent the Pearson correlation coefficient and p-value, respectively, obtained from the linear  
 262 fitting statistics for the respective types of projections.



263  
 264 **Supplementary Figure S24. Cellular morphological diversity among modules.** Sagittal views of randomly selected  
 265 single neuron morphologies within modules, estimated from neurite distribution as discussed in **Figure 2**. The  
 266 dendrites of each neuron are highlighted within the inset dashed rectangle, colored in blue. The axons are represented  
 267 by red lines. The respective neuron types are indicated adjacent to the morphologies. Scale bars are based on the single  
 268 neuron morphologies in each row.